

Fatigue delamination of composite materials – approach to exclude large scale fibre bridging

René Alderliesten

Department of Aerospace Structures and Materials, Faculty of Aerospace Engineering,
Delft University of Technology
Kluyverweg 1, 2629 HS, Delft, The Netherlands

r.c.alderliesten@tudelft.nl

Abstract. This paper proposes a straightforward methodology to generate fatigue delamination curves without the influence of fibre bridging using test data obtained on unidirectional double cantilever beam specimens with fibre bridging.

1. Introduction

Ply delamination growth in laminated fibre reinforced polymer composites has received ample attention in the past decades, as it constitutes a dominant failure mechanism for structures made of these materials. To assess the delamination fracture toughness, subject in quasi-static strength justifications, specimen geometries and test procedures have been standardized for the various opening modes. Take for example for mode I, the double cantilever beam (DCB) test [1]-[2], for mode II the end-notched flexure (ENF) test [3] for mixed-mode I/II, the mixed-mode bending (MMB) test [4].

For fatigue driven delamination growth, however, there is no agreement yet on a standard to correctly obtain fatigue delamination data. Although most researchers adopt standard specimen geometries from quasi-static test standards, no consensus exists on the correct method to test, nor on the proper similitude parameters to adopt [5][6]. Despite that several aspects have been studied through round-robin mode I fatigue fracture tests by both the European Structural Integrity Society Technical Committee 4 and the American Society for Testing and Materials, International, Subcommittee D30.06, a standard has not yet been proposed [7][8][9][10].

Among various factors causing scatter in the data, like e.g. accuracy in load cell and (initial) crack length measurements, it seems that the observed fibre bridging, shielding the crack tip, forms the dominant phenomenon hindering standardization.

Many researchers have studied this phenomenon of fibre bridging. Most studies however, focus on quasi-static loading conditions using critical strain energy release rate (SERR) or stress intensity factors to determine fracture toughness. In that case, large scale fibre bridging contributes to the fracture process zone, which complicates the use of linear elastic fracture mechanics (LEFM). In fatigue delamination growth, these fibres shield the crack tip and store a portion of the applied cyclic load to be released upon unloading. Hence, the application of LEFM may remain more straightforward, as is discussed in this paper.

Fibre bridging appears to be mostly an artefact of testing unidirectional laminates. It occurs in for example DCB laboratory tests, but it is rarely observed and reported for naturally occurring delaminations in operational in-service conditions. This means that fatigue delamination data required



in designing a structure for a given operational life should be conservative in that it excludes fibre bridging.

Hence, most work reported in literature aims to predict the fibre bridging contribution, by quantifying indirectly the magnitude of crack shielding imposed by bridging fibres. It seems though that these indirect methods do not allow to standardize fatigue delamination experiments; to come to delamination resistance curves, data is evaluated through theoretical models, which prohibits treating the data as material data.

This paper therefore discusses a method or approaches to unambiguously account for fibre bridging in mode I fatigue delamination experiments, and to come to conservative delamination resistance curves. First, a brief discussion is given on fibre bridging assessment, data processing and test specification. The paper then proposes a methodology compliant to such specification, demonstrating that material data in the form of delamination resistance curves equivalent to ‘zero bridging’ can be obtained from DCB experiments through a standard test procedure and standard data processing.

2. Assessment of fibre bridging

Literature reports various approaches to evaluate the fibre bridging contribution in mode I quasi-static and fatigue delamination tests. One approach aims at physically removing the bridging fibres [11], while most other approaches attempt to quantify the bridging contribution in order to subtract that from the total work applied. This category can be divided into studies that numerically or analytically model fibre bridging (loads or stresses) [12][13] and studies that attempt to (phenomenologically) correct loading parameters using experimental measurements [9][14][15]. This latter correction is either done with measurements within the same test, or measurements obtained from other tests and specimens.

What all these methods have in common is that the data taken from the experiments is evaluated using theoretical models describing the fibre bridging, which implies that the reported experimental model depends on the appropriateness of the theoretical model adopted. This could be acceptable in the circumstance where everyone agrees to adopt the exact same model, both in processing experimental data and in strength calculations using that data. However, literature evidently has illustrated that many models have been proposed and adopted, each resulting in different delamination growth data. This lack of consensus seems the prime reason for the lack of a standardized fatigue delamination growth test procedure.

3. Data processing and test specification

3.1. Data requirements

Following the discussion on proper similitude [5][6], the fatigue data should contain at least the two parameters that define the entire load cycle, i.e. G_{max} and G_{min} , or G_{max} and ΔG , or G_{max} and $\Delta\sqrt{G} = (\sqrt{G_{max}} - \sqrt{G_{min}})^2$. Here, one should consider that $\Delta\sqrt{G}$ constitutes the best analogy with the stress intensity factor range ΔK proposed by Paris and others [16][17].

From a physical perspective, one should not only consider a ‘driving force’ often described by $\Delta\sqrt{G}$ or ΔG , but also an inherent delamination resistance. Here one could consider the analogy with moving a box over the floor: the movement is described by the applied force minus the effective frictional force between the box and floor. For adhesive fatigue disbond growth, this resistance was observed to correlate well with the maximum work applied, equivalent to G_{max} [18], while the driving force then was described by $\Delta\sqrt{G}$. Hence the two-parameters necessary to describe fatigue delamination growth are not only required to uniquely describe the fatigue load cycle, but also to relate to both a ‘driving force’ and a ‘material resistance’ to the delamination growth rate.

In general, there are two approaches to monitor the crack growth, either visually measuring the length of the crack, or calculating the crack length based on compliance calibration. For generating

fatigue resistance data for design purposes, either approach suffices. However one should keep in mind that the compliance calibration approach is deemed inadequate for proper material interface characterisation, because any discrepancy between crack growth and strain energy dissipation is not captured with an a priori assumed relationship between the two parameters. This is even more the case for mode II fatigue delamination growth where energy dissipates in process zone in front of the crack [19]. Hence, understanding observations on fracture surfaces in SEM investigations, require the visual measurements of the crack lengths, to determine growth rates, rather than calculating them based on compliance. Only then effective delamination resistance expressed as dU/dA can be established.

3.2. Data scatter factors

The crack length a represents the 1-dimensional parameter describing the growth in fracture surface area A . Although for specimen where the thickness or width is constant along the direction of crack growth, theoretically implies a linear relation between a and A , one should keep in mind that change in crack front curvature, or angled crack front in multidirectional laminates might add scatter to crack growth observations.

In that respect, one has to acknowledge the contribution to scatter through fibre bridging in the definition of the pre-crack length [20]. Defining the initial pre-crack length with a tolerance of ± 1 mm, could impose significant scatter in the obtained crack resistance curve. This influence could be reduced following the procedure explained in the next section.

4. Methodology for obtaining ‘zero bridging’ resistance curves

This section outlines a procedure to obtain delamination resistance curves from DCB specimens prescribed in for example [1][2] while eliminating the unavoidable fibre bridging. Although it is recommended here to use $\Delta\sqrt{G}$ as the similitude parameter, one may adopt one of the other earlier mentioned parameters as well.

The main concept underlying the proposed procedure is that eliminating the influence of fibre bridging in a test should require data from that same test specimen only. Hence, the procedure consists of performing multiple fatigue delamination growth tests on the same specimen, which generates multiple crack resistance curves. In the data processing, the data from these curves are evaluated against the effective crack length at which each data point was obtained, and subsequently all data are translated to an effective zero pre-crack length using the relationship against crack length obtained through regression. This procedure can be performed for each specimen individually.

4.1. Experimental procedure

The experimental procedure initially corresponds to what is deemed common practice; the DCB specimen geometry is taken from for example [2]. One should note that the length of the DCB specimen should be sufficiently long to extract at least six to seven curves from that specimen. This could be equivalent to about 70 mm crack extension range [21][22]. Here, it is recommended to adopt the specimen geometry described in [21][22], in which the test procedure has been explained before.

4.1.1. Pre-cracking. Upon manufacturing the laminates for the specimens one has to determine the appropriate thickness, because the thickness has been observed to influence the experimental results [23]. An approximately 12-13 μm thin Teflon or FEP foil should be applied to create the starter crack. This crack is quasi-statically extended several millimetres to create the sharp crack tip. Note that this pre-cracking introduces already a first amount of fibre bridging over the generated pre-crack length.

4.1.2. Fatigue loading. The tests are performed in displacement controlled conditions to achieve stable delamination growth. With the initial maximum displacement equivalent to about 80-90% of the ultimate displacement for quasi-static fracture, the extension in delamination growth reduces the loads and the corresponding SERRs. The test is terminated after the delamination growth retarded, which

may be between 10^{-8} and 10^{-9} m/cycle. Afterwards the fatigue delamination tip is quasi-statically extended another few mm, similar to the pre-cracking procedure. Whether or not this quasi-static pre-cracking is necessary or not, still has to be determined.

The procedure is repeated multiple times, until at least six to seven curves have been obtained covering about 60-70 mm delamination lengths. At these lengths fibre bridging has fully developed as also illustrated by Holmes et al. [24]. Limiting factors for generating multiple curves may be the specimen length, of the maximum machine actuator displacement; the longer the delamination length, the greater the (initial) opening displacement required to achieve the desired G_{\max} . Examples of a set of such curves generated with a single specimen are illustrated in Figure 1.

4.2. Data Evaluation

Paris type power law relationships can be fitted through the curves illustrated in Figure 1 following

$$\frac{da}{dN} = c(\Delta\sqrt{G})^n = c \left[(\sqrt{G_{\max}} - \sqrt{G_{\min}})^2 \right]^n \quad (1)$$

These relationships can be evaluated similar to what is standard practice for $S-N$ fatigue life curves. There, the slope of $S-N$ curves is often described by the Basquin relationship [25], which also constitutes a power law relationship. Hence for each curve in Figure 1, the data points are translated along the slope of equation (1), described by the exponent n , to a selected average value of da/dN . This is illustrated in Figure 2 for the first three curves of Figure 1.

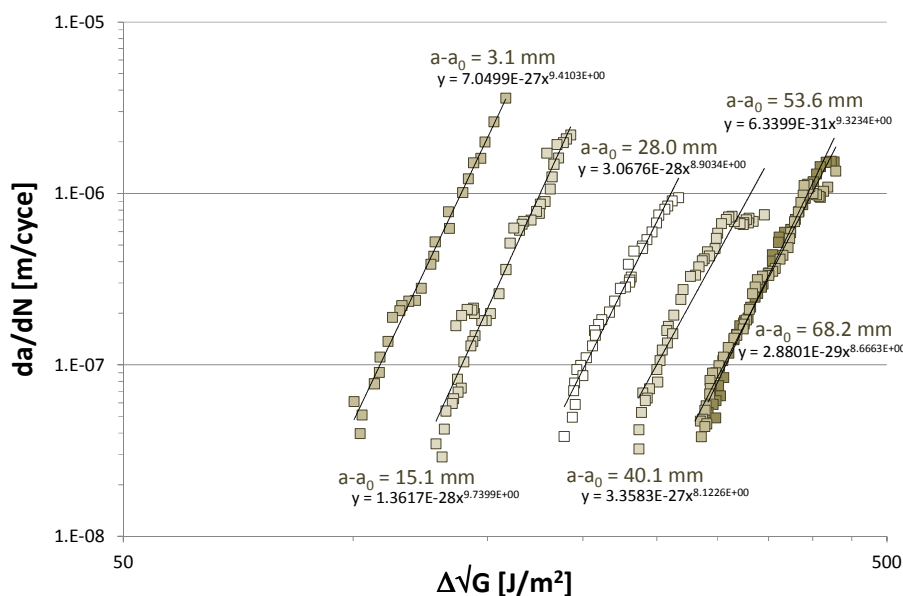


Figure 1. Six successive delamination resistance curves obtained from a single specimen, labelled specimen 7 in [26]

The equation to translate all data points illustrated in Figure 2 is given by

$$\log_{10}(\Delta\sqrt{G}_T) = \frac{1}{n} \left[\log_{10} \left(\frac{da}{dN}_T \right) - \log_{10} \left(\frac{da}{dN} \right) \right] + \log_{10}(\Delta\sqrt{G}) \quad (2)$$

where $\Delta\sqrt{G}_T$ is the value of the SERR after translation, and da/dN_T is the corresponding translated da/dN value. Note that the average value of $\Delta\sqrt{G}_T$ at an arbitrary value of $da/dN = 4.5 \cdot 10^{-7}$ m/cycle plotted against the corresponding crack increment $a-a_0$ yields a nonlinear relationship that either can be approximated with a bilinear presentation [27], or with a second order polynomial function of $a-a_0$. The reason for the curve to approximately become horizontal is attributed to full saturation or full

development of fibre bridging [21]. The increase of fibre bridging in newly created crack lengths is compensated by the pull-out and failure of bridging fibres at the pre-crack side.

Regression analysis. Each data point in Figure 1 corresponds to a specific value of the crack length or $a-a_0$, hence one may fit a surface by regression through $\Delta\sqrt{G}$, $a-a_0$ and da/dN . To enable proper regression, one should first linearize the scales for $\Delta\sqrt{G}$ and da/dN . As mentioned before, the relationship between the crack length $a-a_0$ and $\Delta\sqrt{G}$ appears to be non-linear, as illustrated in Figure 3 for the data in Figure 1.

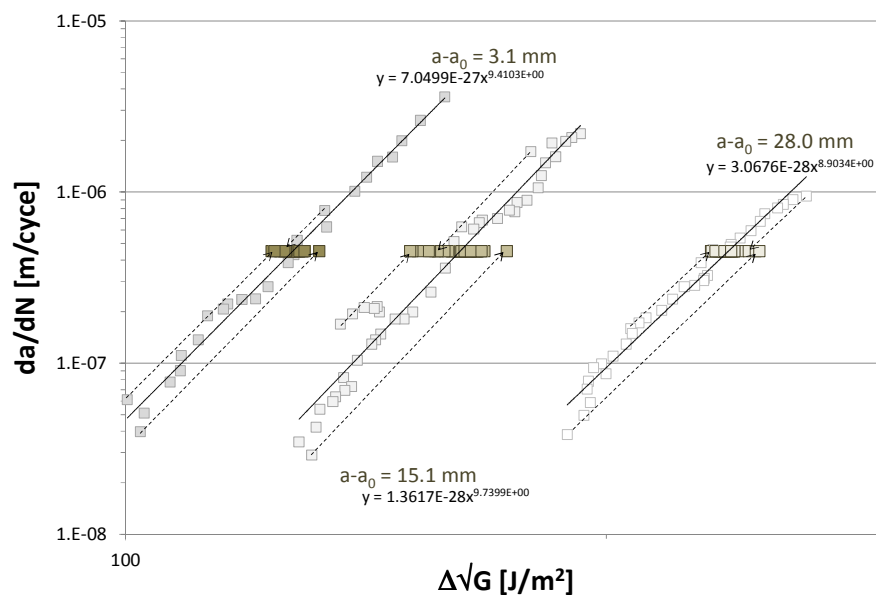


Figure 2. Translating all data along their respective curves to (an arbitrary value of) $da/dN = 4.5 \cdot 10^{-7}$ m/cycle for the first three curves in Figure 1

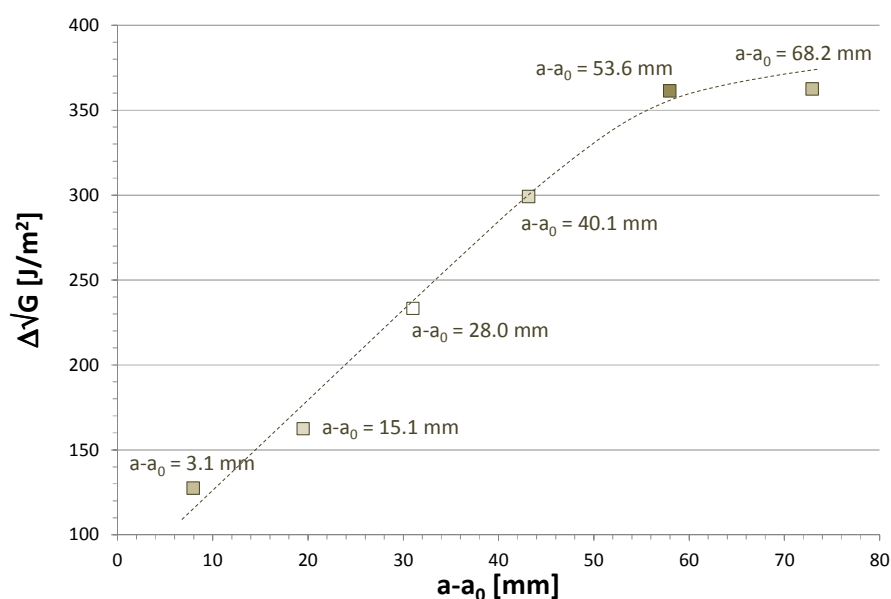


Figure 3. Average crack length at (an arbitrary value of) $da/dN = 4.5 \cdot 10^{-7}$ for the curves in Figure 1

To capture the non-linearity in regression one therefore should verify that sufficient curves have been generated up to the full development of fibre bridging. If that is the case, an appropriate equation for regression is

$$\text{Log}(\Delta\sqrt{G}) = C_0 + C_1(a - a_0) + C_2 \text{Log}\left(\frac{da}{dN}\right) + C_3(a - a_0)^2 + C_4 \left[\text{Log}\left(\frac{da}{dN}\right) \right]^2 \quad (3)$$

where C_i are the constants obtained through regression of all data in Figure 1.

4.2.1. Data quality assessment. The individual curves can be evaluated through comparison of slopes, while data scatter can be analysed for each curve by determining the distribution at the average level of crack growth rate as illustrated in Figure 2. These distributions can be compared, and if necessary (part of) curves may be omitted for having too much scatter.

A straightforward method to obtain a statistical distribution is by ranking the data points obtained after translation to a selected level of da/dN (see Figure 2) from low to high values. Afterwards, a probability P_f (in [%]) can be assigned to each value following [28]

$$P_f = \frac{100n}{n_{tot} + 1} \quad (4)$$

where n is the rank number and n_{tot} is the total number of data points per curve. This allows to plot cumulative density functions for each curve in Figure 1, as illustrated in Figure 4.

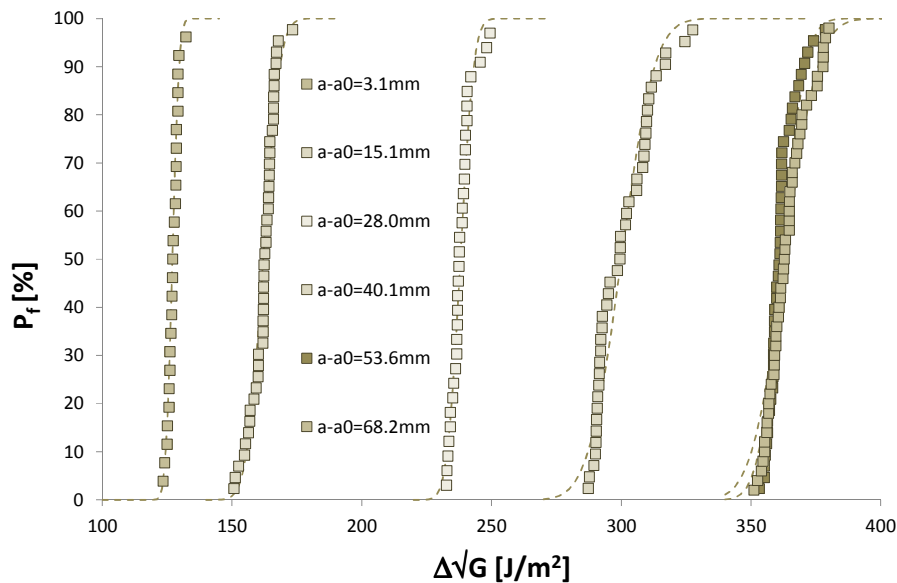


Figure 4. Cumulative density functions at $da/dN = 4.5 \cdot 10^{-7}$ m/cycle for the curves in Figure 1

Theoretically, the zero bridging curve corresponds to a delamination length of $a - a_0 = 0$ mm. Hence, once a surface fit has been obtained through regression using equation (3), the average zero-bridging curve can be described by

$$\text{Log}(\Delta\sqrt{G})_{av,th} = C_0 + C_2 \text{Log}\left(\frac{da}{dN}\right) + C_4 \left[\text{Log}\left(\frac{da}{dN}\right) \right]^2 \quad (5)$$

Obviously, this average curve has limited value in practice, because an upper bound must be established including all material scatter, not only the scatter associated with fibre bridging. Hence, all individual data points must be translated to the zero-bridging curve of equation (5) while maintaining

their relative offset from equation (3). For the curves illustrated in Figure 1, this yields a curve left of all curves as illustrated in Figure 5.

4.3. Reproducibility

To test the reproducibility, first the results of Figure 5 are correlated to the results of another specimen tested under the same test conditions, denoted as specimen 11 in [26]. This specimen has the same material lay-up, specimen configuration and test conditions, including the generation of multiple resistance curves. Few others specimen in [26] have been tested under the same conditions, but only yielding a single resistance curve, or maximum to curves. These will be discussed hereafter.

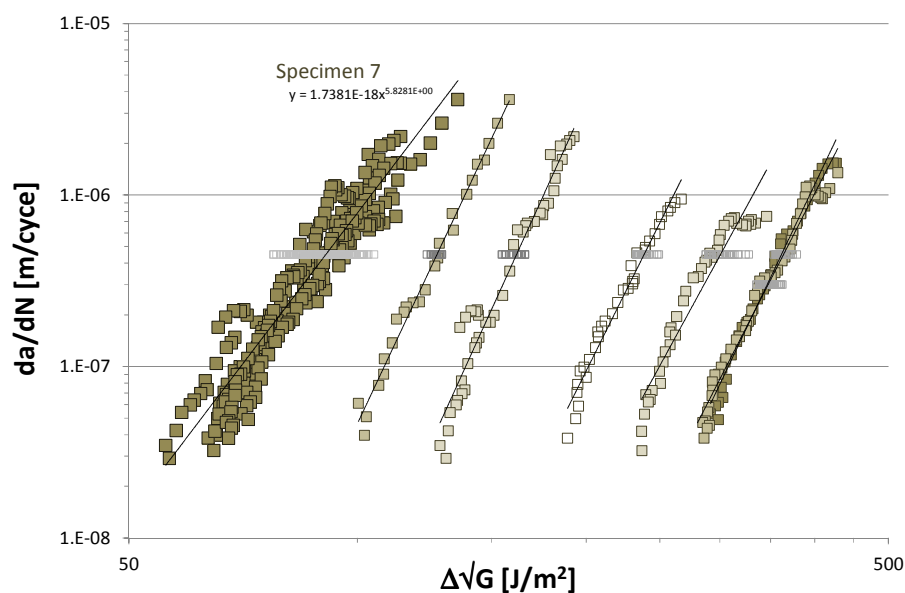


Figure 5. Comparison between the translated curve and the original six curves from specimen 7 in [26]

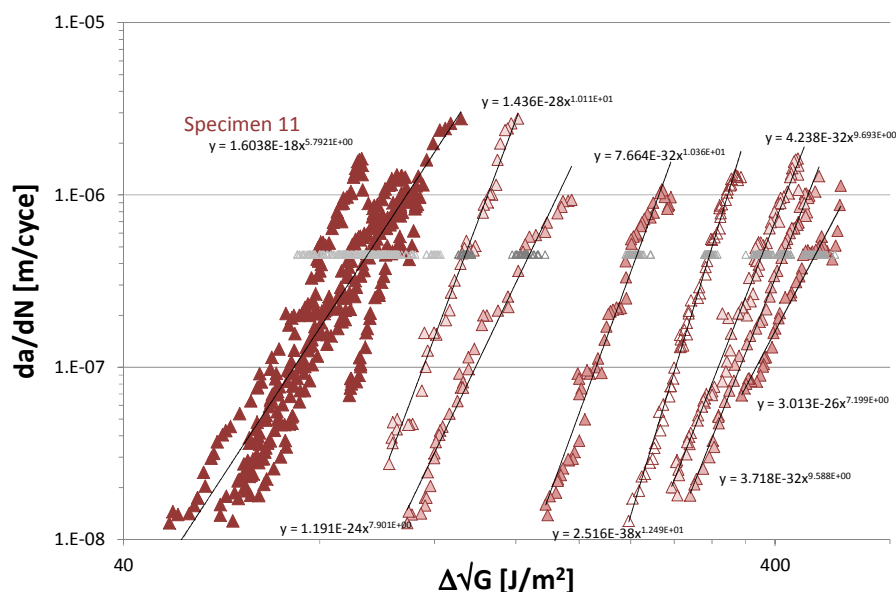


Figure 6. Comparison between the translated curve and seven original curves from specimen 11 in [26]

The obtained resistance curves, with their fit to equation (1), and the curve translated to zero-bridging are presented in Figure 6. To clearly illustrate the excellent correlation between the translated curves from Figure 5 and Figure 6, both are compared in Figure 7. This is further demonstrated by comparing both cumulative density functions for these translated curves in Figure 8. Except for the lower values of $\Delta\sqrt{G}$ both functions correlate very well.

Although a single specimen following the above described procedure yields substantially more data points than traditional single resistance curves, more specimens must be tested to generate so-called A-basis or B-basis allowables [29][30]. For that one must include at least specimens obtained from different material and manufacturing batches.

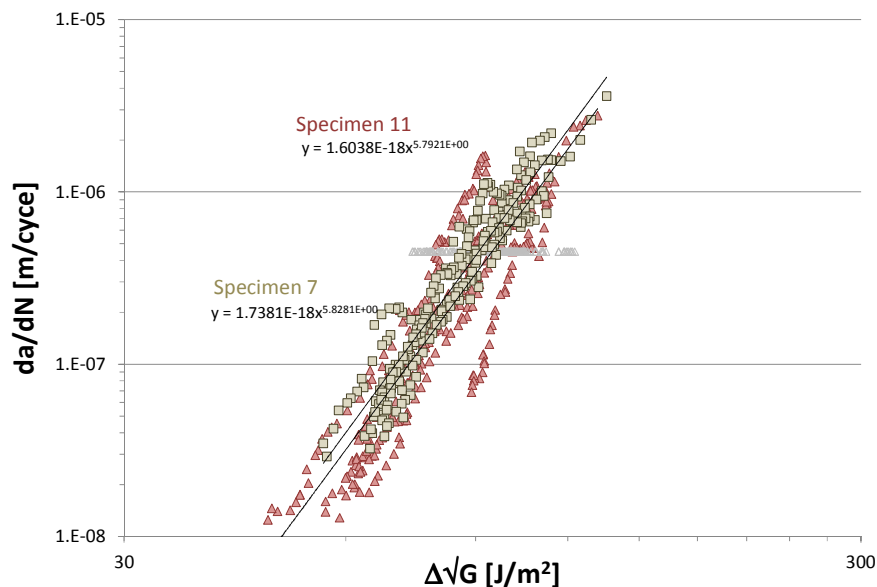


Figure 7. Comparison between the translated curves from Figure 5 and Figure 6

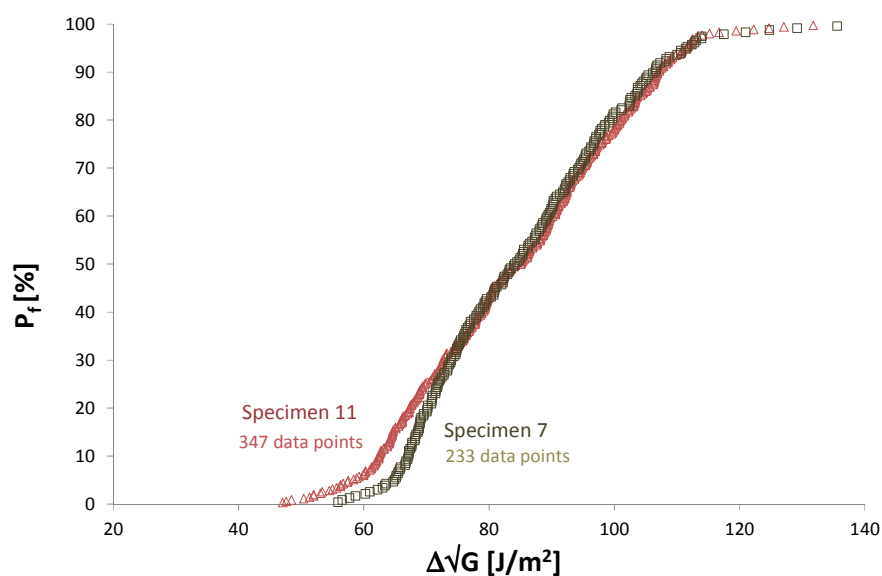


Figure 8. Comparison between the cumulative density functions at $da/dN = 4.5 \cdot 10^{-7}$ m/cycle for the curves in Figure 5 and Figure 6

5. Discussion

5.1. Proper characterisation of behaviour and material variability

The results presented in the previous section show an interesting aspect related to the fatigue delamination resistance curves. All slopes obtained by repeating the test procedure, as illustrated in Figure 5 and Figure 6 exhibit similar steep slopes. However, the translation to zero-bridging curves demonstrate that these slopes are an artefact of fibre bridging in the test. As the test is executed in displacement controlled conditions, the high da/dN data is obtained at the start of the test, while the near threshold data is obtained at the end of the test. As result of crack growth throughout the test, the crack length at the end is greater than the crack length at the start, and thus fibre bridging is also more dominant at the end than at the start. Since bridging moves data (or curves) to higher values of $\Delta\sqrt{G}$, as illustrated in Figure 1, this implies that the slope of the curves end up steeper than they should be without fibre bridging: the upper portion of the curve smoves less to the right than the lower part, effect9vely changing the slope. Without modelling fibre bridging, the above described procedure incorporates this effect, and yields a zero-bridging resistance curve less steep than all the original curves.

Another observation one can make is that the scatter or variability in the original individual curves are smaller than the scatter in the translated zero-bridging curve. Here, one has to keep in mind that technically with each repetition of the test procedure to obtain multiple cures from a single specimen conditions change. Material variability will appear in the variation of fibre bridging and thus the magnitude of crack tip shielding effectively, which is included when translating all curves to $a-a_0 = 0$.

Here, one could argue that the material variability one seeks to obtain with testing multiple specimens, to some extent is also obtained with testing the same specimen multiple times. In any case, because of the relatively large amount of data points in the zero-bridging resistance curve, statistical methods can be adopted to establish upper bounds with sufficient confidence. Nonetheless, as mentioned before, this procedure does not eliminate the need to test multiple specimens for defining design allowables.

5.2. Limiting conditions to the proposed procedure

This procedure explained above constitutes a straightforward methodology to derive zero-bridging delaminations resistance curves without requiring theoretical models to describe the fibre bridging. Here one should note that recently Yao et al. [23] demonstrated specimen thickness has no significant effect on the zero-bridging curve. This may seem counter intuitive considering the thickness effects reported for quasi-static loading [12][31].

Nonetheless, one has verify whether certain conditions are met before applying the procedure. Take for example the earlier mentioned tests reported in [26], where only one or two delamination resistance curves were generated. For both specimens the two original resistance curves are plotted against the translated zero-bridging curves in Figure 9.

Evidently, the zero-bridging curves for specimens 1 and 2 do not coincide, nor do they correlate well with the zero bridging curves for specimens 7 and 11 illustrated in Figure 7. This can be best explained with looking at the regression equation, equation (3) and the trend illustrated in Figure 3. Since both specimen 1 and 2 comprise two curves, they effectively form each two data points through which a non-linear regression is performed. Hence, two justify the regression of equation (3), one needs at least a certain amount of resistance curves ranging over sufficient crack lengths $a-a_0$, to capture a non-linear relationship as illustrated in Figure 3. Simply one or two resistance curves will not work.

As a solution to the inapplicability of the methodology to data comprising too few curves, one could consider combining all data and applying the procedure to the combined data set. The reasoning then may be that the original resistance curves in Figure 9 all correlate to specific crack length (for

specimen 2 even up to $a-a_0 = 89.6$ mm), which altogether contain sufficient range for the regression with equation (3).

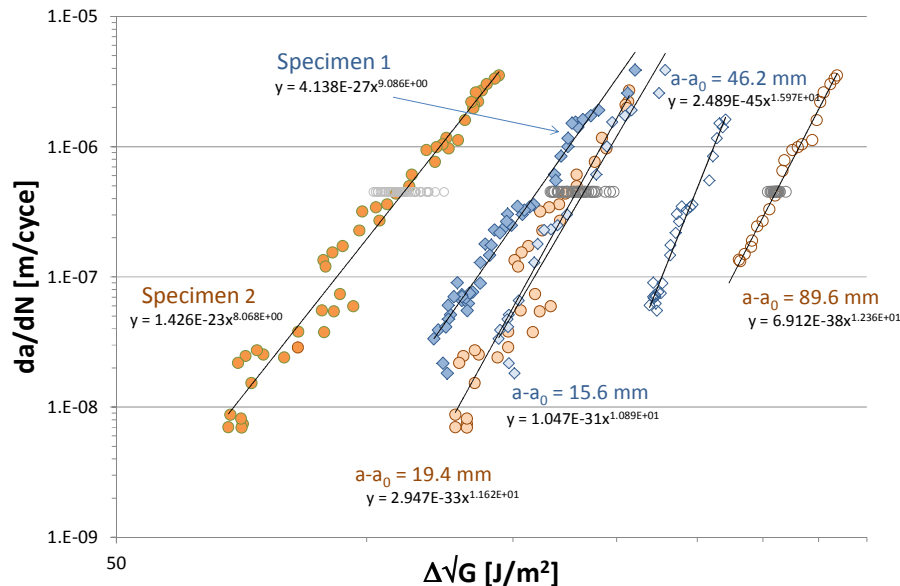


Figure 9. Comparison between the translated curves and two original curves from specimens 1 and 2 in [26]

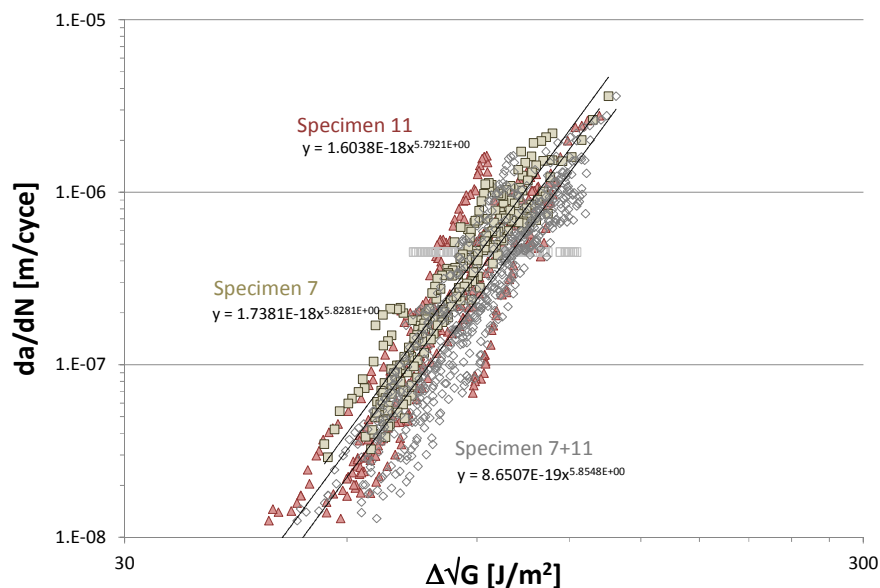


Figure 10. Comparison between the translated curve obtained after regression through the combined data from specimen 7 and 11 with the individual translated curves from Figure 7

To test whether such combined approach is valid, the data from specimens 7 and 11 in [26] can be used. Rather than performing regression per specimen, resulting in the delamination resistance curves shown in Figure 7, all data of both specimens could be combined after which the regression is performed on the total data set. The zero-bridging delamination resistance curves obtained after regression on both datasets combined is compared with the curves from Figure 7.

What is apparent from Figure 10 that the data points obtained with regression through the combined dataset does not overlay the data points obtained with regression through the individual data sets. It appears that the curve has moved slightly to the right compared to the curves from Figure 7. This can be further illustrated by comparing the cumulative density function of the curve with the individual curves shown in Figure 8.

It is evident that performing the regression on the combined dataset rather than the individual datasets, can yield a delamination resistance curve of which the upper bound is moved to the right. Compared to the original curves in Figure 8 this implies an unconservative curve. Whether this interaction between the two datasets relates to the crack growth rate da/dN , the SERR $\Delta\sqrt{G}$, or the crack length $a-a_0$ has yet to be further investigated.

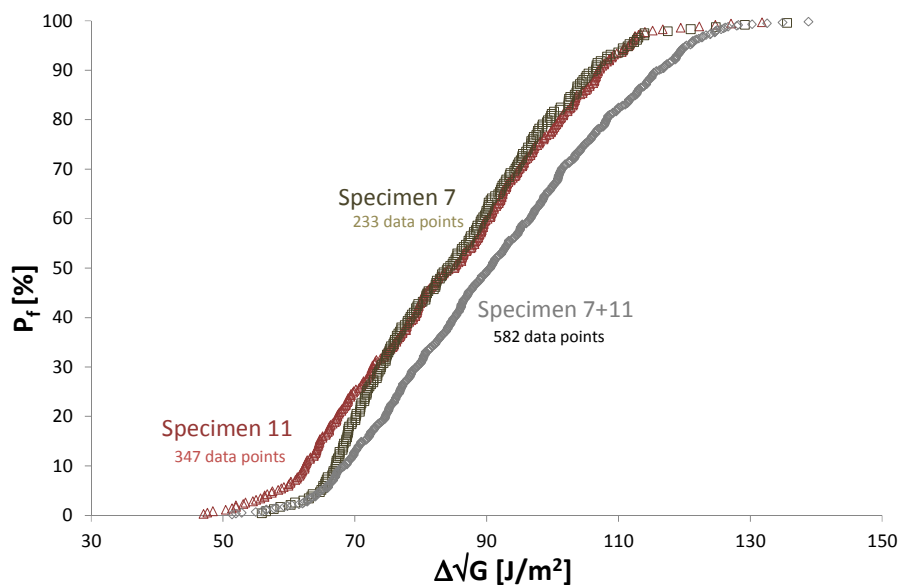


Figure 11. Comparison between the cumulative density functions at $da/dN = 4.5 \cdot 10^{-7}$ m/cycle for the curve obtained with regression to the combined dataset and the curves from Figure 8

5.3. Ways forward to standardization

What the above explained procedure and the corresponding data and results have demonstrated is that it is very well possible to generate fatigue delamination resistance curves without the influence of fibre bridging while testing unidirectional laminated composites. Simply taking the DCB specimen and repeating the tests multiple times yields data that can be evaluated without requiring a theoretical model for fibre bridging.

However, the presented results also illustrate that care has to be taken that certain conditions are met before one can claim that the data is valid. The advantage of the presented approach, however, is that straightforward verification is available. One can verify whether the multiple curves obtained exhibit the non-linear relation illustrated in Figure 3 to capture fibre bridging development up to full saturation. One can also assess the individual slopes of the curves or distributions by comparing all distributions based on their individual cumulative density functions as demonstrated in Figure 4.

Translating all curves per specimen to a zero-bridging curve allows comparison between different specimens, to verify whether indeed all specimens exhibit the same delamination resistance curves, like shown in Figure 7 and Figure 8. Combining all individual zero-bridging curves will then allow the application for statistical methods to establish A-basis or B-basis upper bounds for strength justification.

The question left to answer is how to exploit all existing data that in most cases represent single delamination resistance curves per specimen. Following the approach proposed here, one needs to take the specimens and continue testing to generate the other resistance curves. However, if the specimens are no longer available, either because specimens have been taken apart for post-mortem investigations, or because specimens have been thrown away, data might still be used.

This is demonstrated recently in [32] using the same dataset from [26] but evaluated with the Hartman-Schijve relationship [33] proposed previously by Jones et al. [34][35] [36]. All data obtained on different specimens, tested under different loading conditions, collapse together when evaluated with the Hartman-Schijve relationship, yielding a similar curve as the zero-bridging curve presented here. The position and slope of the curve in [32] seems to agree rather well with the curves presented here, which indicates there are more ways to verify the validity of delamination resistance curves.

This seems further illustrated by Yao et al. [27] when proposing an alternative effective SERR parameter after [37], defined as

$$\Delta G_{eff} = \left(\sqrt{G_{tip}^{max}} - \sqrt{G_{tip}^{min}} \right)^2 \quad (6)$$

with

$$G_{tip} = \frac{G_0}{G_{IC}(a - a_0)} G_{applied} \quad (7)$$

where G_0 is derived from extrapolating the trend illustrated in Figure 3 back to $a - a_0 = 0$, while the denominator relates to any point on the trend line of Figure 3. This approach is very simple, and technically performs an analogous or similar procedure as proposed above. It also appears that the zero-bridging curves obtained with this method correlate rather well with the zero-bridging curves presented for example in Figure 7.

The main difference at this moment is in the formulation of the trend in for example Figure 3. Here, it is assumed to represent a polynomial relationship gradually developing to a horizontal asymptote imposed by full fibre bridging development, while in [27] a bilinear relationship is assumed. Further scrutiny of the results is required to decide which type of relationship is preferred before fatigue delamination experiment can be standardized following these procedures.

Here the dataset from [26] might allow a first step into such study, because both 0//0 and 45//45 interface configurations have been adopted. As examined in [38], the amount of fibre bridging associated with these two interface types is substantially different. Hence, both methods of extrapolating or translating data to zero-bridging curves can be applied to these interfaces to investigate whether both interfaces yield similar zero-bridging curves. Nonetheless, one has to consider the possibility that still different curves are obtained, which may then relate to different fracture morphology or crack branching.

6. Conclusions

This paper presents an approach to determine upper bound fatigue delamination resistance curves obtained with tests on unidirectional laminated DCB specimens. The fibre bridging generally observed to occur in these specimen configurations is eliminated with the proposed methodology. The paper discusses some conditions that must be verified before the methodology yields valid results, and it demonstrates how the approach correlates with other approaches proposed in literature.

Acknowledgement

The author wishes to express his gratitude to Liaojun Yao and John-Alan Pascoe for the many fruitful and stimulating discussions during and after their PhD research performed under the author's supervision.

References

- [1] ASTM D5528-01. *Standard test method for mode I interlaminar fracture toughness of unidirectional fiber-reinforced polymer matrix composites.*
- [2] ASTM D6115-97. *Standard test method for mode I fatigue delamination growth onset of unidirectional fiber-reinforced polymer matrix composites.*
- [3] ASTM D7905/D7905M-14. *Standard Test Method for Determination of the Mode II Interlaminar Fracture Toughness of Unidirectional Fiber-Reinforced Polymer Matrix Composites.*
- [4] ASTM D6671/6671M-06. *Standard test method for mixed mode I-Mode II interlaminar fracture toughness of unidirectional fiber reinforced polymer matrix composites.*
- [5] Rans CD, Alderliesten RC, Benedictus R 2011, *Misinterpreting the results: How similitude can improve our understanding of fatigue delamination growth*, Compos Sci Technol 71: 230–238.
- [6] Alderliesten RC 2015, *How proper similitude principles could have improved our understanding about fatigue damage growth*, Proceedings of the 28th ICAF Symposium – Helsinki, 3–5 June 2015.
- [7] Brunner AJ, Murphy N, Pinter G 2009 *Development of a standardized procedure for the characterization of interlaminar delamination propagation in advanced composites under fatigue mode I loading conditions*, Eng Fract Mech 76: 2678–2689
- [8] Stelzer S, Brunner AJ, Argüelles A, Murphy N, Pinter G 2012, *Mode I delamination fatigue crack growth in unidirectional fiber reinforced composites: Development of a standardized test procedure*, Compos Sci Technol 72: 1102-1107
- [9] Murri GB 2014, *Effect of data reduction and fiber-bridging on Mode I delamination characterization of unidirectional composites*. J Compos Mater 48: 2413-2424
- [10] Stelzer S, Brunner AJ, Argüelles A., Murphy N, Cano GM, Pinter G 2014, *Mode I delamination fatigue crack growth in unidirectional fiber reinforced composites: Results from ESIS TC4 round-robins*, Eng Fract Mech 116: 92-107
- [11] Khan R, Alderliesten RC, Yao L, Benedictus R 2014, *Crack closure and fibre bridging during delamination growth in carbon fibre/epoxy laminates under mode I fatigue loading*, Comp: Part A 67: 201–211.
- [12] Spearing SM, Evans AG 1992, *The role of fibre rbridging in the delamination resistance of fiber-reinforced composites*, Acta metall, mater. 40(9): 2191-2199
- [13] Daneshjoo Z, Shokrieh MM, Fakoor M 2018, *A micromechanical model for prediction of mixed mode I/II delamination of laminated composites considering fiber bridging effects*, Theoretical and Applied Fracture Mechanics 94: 46–56.
- [14] Jones R, Pitt S, Brunner AJ, Hui D 2012, *Application of the Hartman-Schijve equation to represent Mode I and Mode II fatigue delamination growth in composites*. Compos Struct 94: 1343-1351.
- [15] Murri GB 2013, *Evaluation of delamination onset and growth characterization methods under mode I fatigue loading*, Langley Research Center, Hampton, Virginia. NASA/TM-2013-217966.
- [16] Paris PC, Gomez RE, Anderson WE 1961, *A rational analytic theory of fatigue*, The Trend in Engineering, 13(1): 9-14.
- [17] Paris PC, Erdogan F, 1963, *Critical analysis of crack growth propagation laws*. ASME Transactions Journal Basic Engineering, 85D: 528-534.
- [18] Pascoe JA, Alderliesten RC, Benedictus R 2017, *On the physical interpretation of the R-ratio effect and the LEFM parameters used for fatigue crack growth in adhesive bonds*, Int J Fatigue 97: 162–176.
- [19] Amaral L, Zarouchas D, Alderliesten RC, Benedictus R 2017, *Energy dissipation in mode II fatigue crack growth*, Eng Fract Mech 173: 41–54
- [20] Alderliesten RC, Brunner AJ, Pascoe JA (2018), *Cyclic fatigue fracture of composites: What*

- has testing revealed about the physics of the processes so far?*, Eng Fract Mech, submitted
- [21] Yao L, Alderliesten RC, Zhao M, Benedictus R 2014, *Discussion on the use of the strain energy release rate for fatigue delamination characterization*, Composites: Part A 66: 65–72
 - [22] Yao L, Alderliesten RC, Benedictus R 2016, *The effect of fibre bridging on the Paris relation for mode I fatigue delamination growth in composites*, Compos Struct 140: 125–135.
 - [23] Yao L, Cuib H, Alderliesten RC, Suna Y, Guoao L 2018, *Thickness effects on fibre-bridged fatigue delamination growth in composites*, Composites Part A 110: 21–28
 - [24] Holmes JW, Liu L, Sørensen BF, Wahlgren S 2014, *Experimental approach for mixed-mode fatigue delamination crack growth with large-scale bridging in polymer composites*, Journal of Composite Materials. 48: 3111–3128
 - [25] Schijve J 2009, *Fatigue of Structures and Materials*, 2nd edition, Springer Science + Business Media.
 - [26] Yao L, Alderliesten RC 2014, *Mode I fatigue delamination growth in composite laminates with fibre bridging— datasets, collection of datasets*; Available at: <http://dx.doi.org/10.4121/uuid:6da548f6-f801-41b4-8d88-db9ae81f6913>.
 - [27] Yao L, Sun Y, Guo L, Zhao M, Jia L, Alderliesten RC, Benedictus 2017, *A modified Paris relation for fatigue delamination with fibre bridging in composite laminates*, Compos Struct 176: 556–564
 - [28] Van Lipzig H 2016, *Spreiding bij Vermoeiing en Levensduur*, Hoofdstuk 12 PAO cursus Vermoeiing van Constructies, PAO Techniek en Management, Delft www.paotm.nl (in Dutch).
 - [29] Niu MCY 1992, *Airframe structural design, Practical Design Information and Data on Aircraft Structures*, Conmilit Press Ltd, Hong Kong
 - [30] Composite Materials Handbook CMH-17, Volume 1. Polymer Matrix Composites: Guidelines for Characterization of Structural Materials, 2012
 - [31] Suo Z, Bao G, Fan B 1992, *Delamination R-curve phenomena due to damage*, J. Mech. Phys. Solids. 40: 1–16.
 - [32] Yao L, Alderliesten RC, Jones R, Kinloch AJ 2018, *Delamination Fatigue Growth in Polymer-Matrix Fibre Composites: A Methodology for Determining the Design and Lifting Allowables*, Compos Struct 196: 8–20.
 - [33] Hartman A, Schijve J 1970, *The effects of environment and load frequency on the crack propagation law for macro FCG in aluminum alloys*, Eng Fract Mech 1:615–631.
 - [34] Jones R, Pitt S, Brunner AJ, Hui D 2012, *Application of the Hartman-Schijve equation to represent Mode I and Mode II fatigue delamination growth in composites*. Comp Struct 94: 1343–1351.
 - [35] Jones R, Hu W, Kinloch AJ 2015, *A convenient way to represent FCG in structural adhesives*, Fatigue Fract Eng M 38, 2015: 379–391.
 - [36] Jones R, Kinloch AJ, Michopoulos JG, Brunner AJ, Phan N 2017, *Delamination growth in polymer-matrix fibre composites and the use of fracture mechanics data for material characterisation and life prediction*, Compos Struct 180: 316–333
 - [37] Donough MJ, Gunnion AJ, Orifici AC, Wang CH 2015, *Scaling parameter for fatigue delamination growth in composites under vary loading ratios*, Compos Sci Technol 120: 39–48.
 - [38] Yao L, Alderliesten RC, Zhao M, Benedictus R 2014, *Bridging effect on mode I fatigue delamination behavior in composite laminates*, Composites: Part A 63: 103–109